METROLOGY AND MEASUREMENT SYSTEMS

Index 330930, ISSN 0860-8229

www.metrology.wat.edu.pl

IMPROVING THE EFFICIENCY OF SOFT ELECTRON IONIZATION BY USING THE OSCILLATORY MOVEMENT OF ELECTRONS

Ze-Jian Huang[1], You Jiang[1], Xin-Hua Dai[1], Ming-Fei Zhou[2], Xiang Fang[1]

1) *National Institute of Metrology, 18, Beisanhuandonglu, Chaoyang District, Beijing, 100029, P.R. China* (✉ *huangzj@nim.ac.cn*)
2) *Fudan University, Department of Chemistry Jiangwan Campus, HuaXue Building A3002, Shanghai, 200433, P.R. China*

Abstract

In process analytical chemistry, mass spectrometry analysis using soft electron ionization (EI) source has qualitative advantages. However, the relatively small ionization cross-section of soft EI leads to lower sensitivity. To address this issue, a novel method has been developed to enhance the sensitivity of soft EI by utilizing a dual electron repeller and an ionization chamber to form a U-shaped electric field, causing electrons to oscillate within the field and effectively increasing the electron collision cross-sectional area. By combining with an electron lens, the virtual cathode effect at low electron energy can be reduced or even eliminated, thereby improving ionization efficiency. This method has resulted in a significant increase in signal intensity for m/z 18(H_2O), with a factor of 4.2 at an electron energy of 25 eV and a factor of 3.75 at 20 eV, compared to the electron receiving mode. Additionally, it reduces the required emission current, which is beneficial for prolonging the life of the filament. The proposed technique is expected to expand the application of soft EI, particularly for rapid online analysis in process analytical chemistry such as catalyst research and chemical reaction process monitoring.

Keywords: online mass spectrometer, soft electron ionization, electron oscillation, virtual cathode.

1. Introduction

Mass spectrometry (MS) is a widely used technique in process analysis due to its high sensitivity, specificity, fast detection, and strong qualitative ability. The core of MS analysis is the detection of ions, which are charged particles formed when molecules, atoms, or atomic groups lose or gain one or more electrons. Therefore, ions are essentially another form of molecules, atoms, or atomic groups, such as molecular ions, protonated molecular ions (M^+ and $[M+H]^+$), fragment ions (M_1^+ and M_2^+), and adduct ions ($[M+NH_4]^+$ and $[M+Na]^+$). Since these ions represent the structural information of the substance, MS has strong qualitative capabilities. Additionally, the abundant data available in mass spectrometry libraries can be utilized for compound identification.

When ionization occurs, all substances in a sample are ionized simultaneously. This results in the entry of ions of varying mass-to-charge into the mass analyzer, which poses a significant challenge for analysis. Due to the potential overlap of molecular ions and fragment ions from different substances, mass spectrometry may struggle to distinguish between ions from different sources, making qualitative and quantitative analysis difficult. One way to solve this problem is to use tandem techniques, such as combining chromatography with mass spectrometry, like *gas chromatography-mass spectrometry* (GC-MS). The mixture is first separated by gas chromatography and then detected by mass spectrometry. However, this method may not be suitable for real-time detection due to the time required for separation. Another popular way to avoid overlapping is to use soft ionization technology, which has low ionization energy and detects only molecular ions without interference from fragment ions. This results in simple and

easy-to-distinguish MS peaks, making it easier to perform qualitative analysis by molecular weight.

Soft ionization technology encompasses various techniques such as *Chemical Ionization* (CI)[1–4], *Electrospray Ionization* (ESI)[5–8], *Atmospheric Pressure Chemical Ionization* (APCI)[9–14], *Desorption Electrospray Ionization* (DESI))[15–17], *Direct Analysis in Real Time* (DART)[18–23], *Dielectric Barrier Discharge Ionization* (DBDI)[24–26], and *Single Photon Ionization* (SPI)[27–31]. However, CI is not suitable for online industrial applications due to its reliance on a reaction gas and inferior stability compared to EI. Similarly, ESI and other soft ionization technologies are primarily used for polar molecules, making them unsuitable for detecting nonpolar and weak polar small molecules in online industrial settings. Currently, EI remains the primary ionization source in online industrial analysis. While EI works efficiently at 70 eV hard ionization mode, its ionization energy can be easily adjusted to operate in soft ionization mode [32–37]. Nonetheless, as electron energy decreases, the sensitivity of the EI source also diminishes accordingly.

The fundamental principle of EI source is to accelerate electrons that overflow from a hot cathode under the influence of an electric field. These electrons then collide with molecules in the gas phase, leading to their ionization. This interaction between electrons and molecules is a fundamental process in collision physics. Due to its significance in collision dynamics and practical applications, numerous theoretical and experimental studies have been conducted on this process. For instance, at the end of the 20th century, Ehrhardt [38] and Straub [39–41] carried out experiments on electron energy and collision cross-sections with various gas molecules. In 2000, Deutsch summarized the progress in theoretical calculations of the electron impact ionization cross-section area [42]. The results indicated that the effective collision cross-section of electrons and gas molecules decreases when the electron energy is low, reducing the probability of gas molecule ionization and ionization efficiency. This phenomenon occurs because EI source operates in a low-energy mode, resulting in a reduced collision cross-section area and weakened ionization efficiency. Consequently, soft EI applications in mass spectrometry are rarely reported.

The collision cross-section is the parameter for a single collision between each electron and molecule. Increasing the number of collisions between electrons and molecules is equivalent to increasing the collision cross-section of a single electron. Consequently, increasing the number of collisions can enhance the probability of electron collision ionization, thereby improving the utilization rate of electrons and consequently, the ionization efficiency.

This research proposes a novel method for developing a soft EI source with enhanced sensitivity. The proposed approach employs a U-shaped electric field to oscillate electrons back and forth within the ionization chamber, thereby extending the length of their motion path. This increases the probability of collisions between electrons and gas molecules, effectively increasing the collision cross-sectional area of electrons, and consequently improving the sensitivity of mass spectrometry. However, as electron energy decreases, the electric field force acting on electrons weakens, causing their velocity to slow down. Consequently, electrons fail to reach the anode, forming a spatial barrier near the surface of the hot cathode known as the "virtual cathode"[43-48]. This virtual cathode significantly impedes the movement of electrons towards the interior of the ionization chamber, adversely affecting ionization efficiency. In this study, the impact of virtual cathode was eliminated by incorporating an electron lens. This led to a substantial enhancement in signal intensity for m/z 18 (H2O), with a factor of 4.2 at an electron energy of 25 eV and a factor of 3.75 at 20 eV, as compared to the electron receiving mode. This technology can significantly improve ionization efficiency at low electron energies, making soft EI more practical.

2. Experimental section

The experiment is based on a custom-built fast online mass spectrometer [49] (Fig. 1). The EI source features a cross-beam structure with dual filaments, where the two filaments are positioned relative to each other. Each filament is equipped with an electron repeller that propels electrons towards the ionization chamber. Two magnets are respectively placed outside the two filaments to form a magnetic field coaxial with the direction of electron motion. The profile of the EI source is shown in Fig. 2.
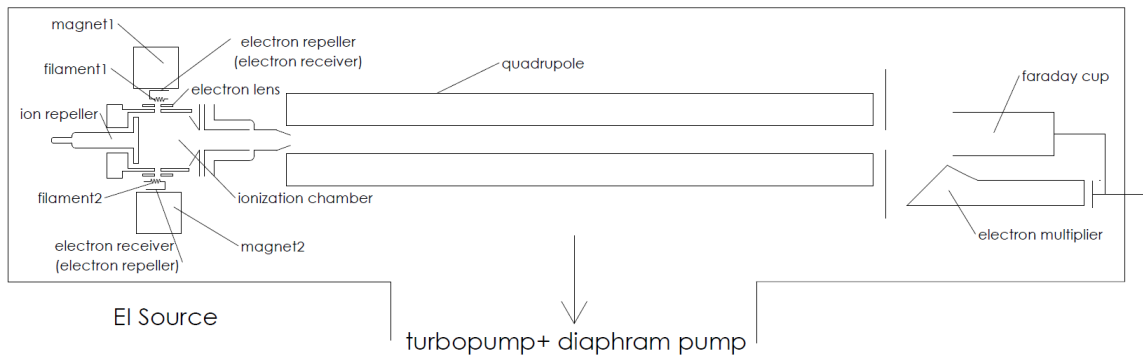

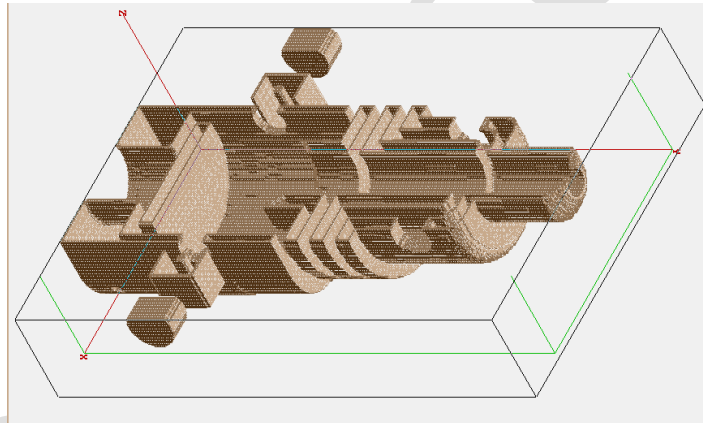Fig. 1. Structure diagram of custom-built fast online mass spectrometer.

Fig. 2. Structure diagram of the EI source.

These two filaments do not operate simultaneously. While one filament is active, the other can function in either the electron reception mode or the electron repulsion mode. In the electron reception mode, the electron repeller is grounded, and a microampere meter is connected in series to measure the received electrons. The movement of electrons is simulated using SIMION 2020, and the results indicate that in this mode, electrons are emitted from the activated filament and spiral along the direction of the magnetic field before being received by the receiving electrode. The single-electron movement simulation diagram and electron trajectory diagram are presented in Fig. 3a and Fig. 3a, respectively.

Conversely, in the electron repulsion mode, the electron repellers of both filaments are short-circuited. The electron repeller has a lower voltage compared to the inner wall of the ionization chamber, creating a U-shaped electric field. However, a mere U-shaped electric field is insufficient to enable electrons to oscillate back and forth within it sufficiently. The motion direction of electrons will become increasingly divergent if it is not restricted, and they will soon collide directly with the walls of the ionization chamber and disappear. However, under the influence of a magnetic field, electrons are confined within a spiral

radius and move in a spiral motion along the direction of the magnetic field. Simulation results show that the spiral radius is on the micrometer scale, so it can be considered that electrons move linearly along the magnetic field. Under the combined influence of the U-shaped electric field and the magnetic field, electrons undergo oscillatory motion until they eventually collide with the ionization chamber and disappear. The movement of a single electron in the ionization chamber is depicted in Fig. 3c and Fig. 3d, which show its trajectory and simulation diagram. The results indicate that the electron oscillates numerous times within the chamber, with hundreds of cycles observed. The speed at which the electron moves within the chamber is illustrated in Fig. 4, showing acceleration, constant velocity, deceleration, and then reversing these movements until it ultimately collides with the chamber walls and ceases to exist.
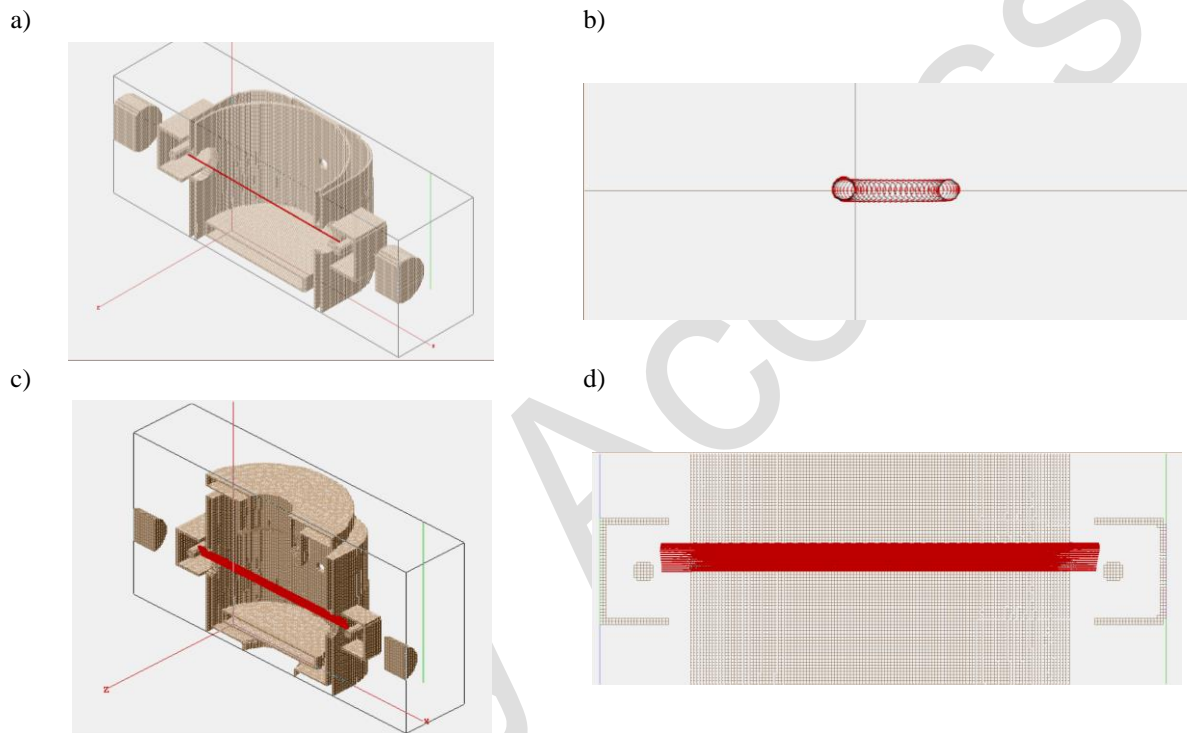
a)

b)

c)

d)

Fig. 3. a) Simulation diagram in the electron reception mode. b) Trajectory diagram of a single electron in the electron reception mode. c) Simulation diagram in the electron repulsion mode. d) Trajectory diagram of a single electron in the electron repulsion mode.
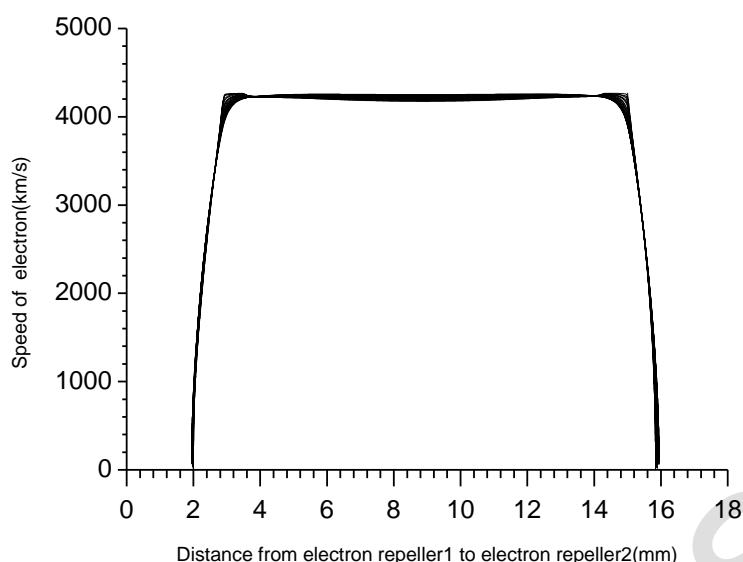
Fig. 4. Schematic diagram of electron motion within the ionization chamber.

At low electron energy, that virtual cathode cause a rapid decrease in sensitivity. To eliminate or even reduce the effect of the virtual cathode, an electron lens is incorporated between the filament and the ionization chamber, featuring a circular aperture at its center. By adjusting the working voltage applied on the electron lens, electrons can enter and pass through the ionization chamber normally. Subsequently, under the influence of the reverse accelerating electric field applied on the nonworking filament electron repeller, electrons return to the ionization chamber. The resulting oscillation of electrons back and forth within the ionization chamber enhances ionization efficiency.

The mass filter is a quadrupole with $\Phi 6$ mm $\times$ 115 mm. Following this, there is a continuous channel electron multiplier equipped with a Faraday cup.

The application of low electron energy EI source is one of the important purposes to remove gas chromatography, which can realize fast and direct real-time analysis of gas samples or real-time detection of residual gases. In order to reduce the fluctuations in measurement data caused by unstable airflow in the injection system, the experiment is mainly conducted in a closed vacuum chamber with a background gas consisting mainly of residual water vapor.

3. Results and discussion

3.1. Experimental comparison of electron oscillation and non oscillation at an electron energy of 70 eV

The variation of the MS peak intensity of m/z 18 (H_2O) with changes in filament emission current under electron reception mode (<18.5 minutes) and electron repulsion mode (>20 minutes), with an electron energy of 70 eV, is shown in Fig. 5a. When the nonworking filament operates in electron receiving mode, the intensity of m/z 18 gradually increases with the filament emission current. Upon reaching a filament emission current of 520 µA, the intensity of m/z 18 reaches its maximum value of 640 mV. If the filament emission current continues to increase, the MS peak intensity will not increase but slightly decrease. In contrast, when the nonworking filament operates in electron repulsion mode, only a few microamperes of emission current are required to achieve a MS peak intensity of 920 mV.
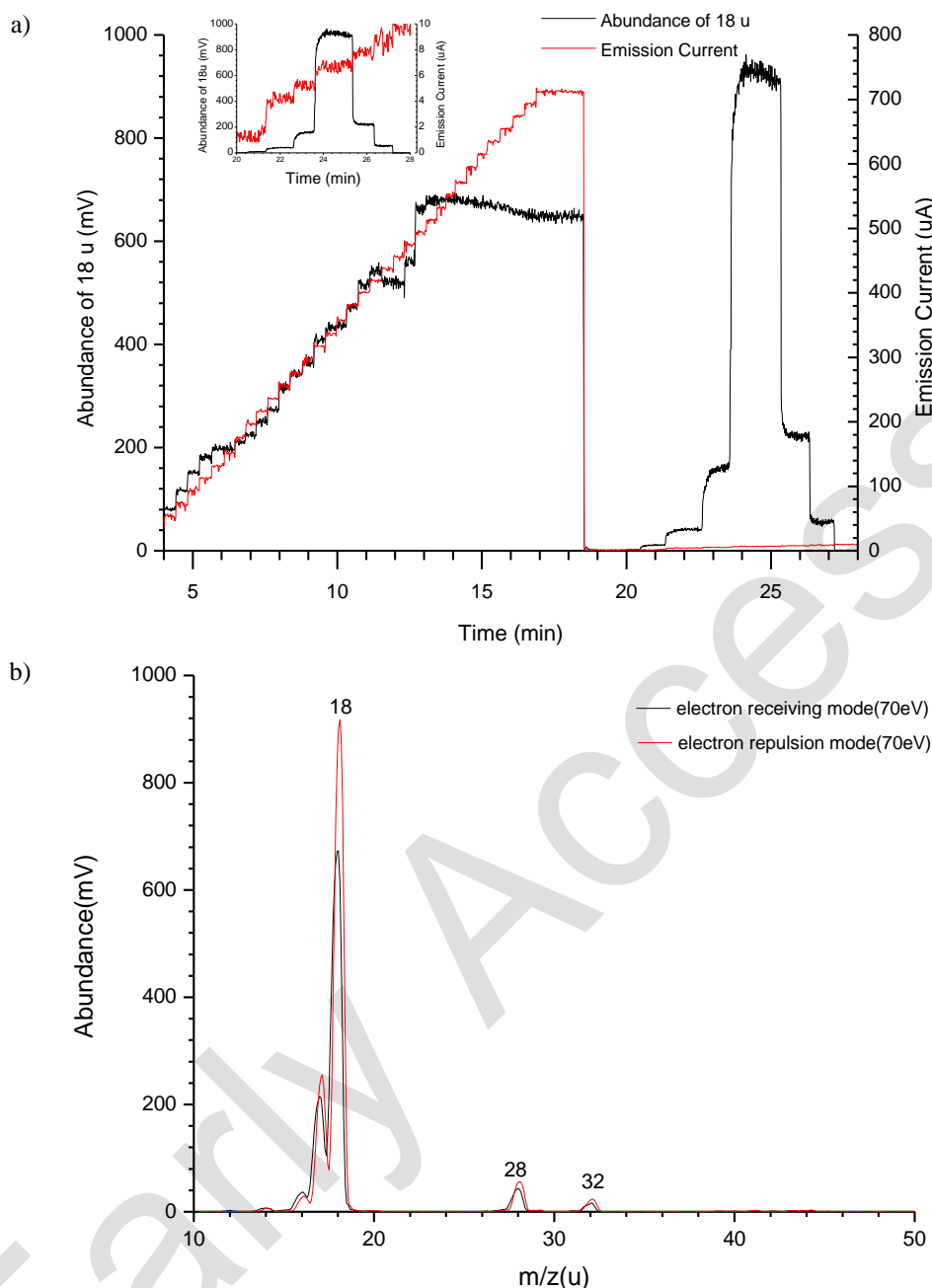
Fig. 5. a) The curve of the filament emission current and m/z 18 intensity at 70 eV (electron receiving mode (< 18.5 min) and electron repulsion mode (> 20 min). b) Comparison of MS peak intensity in electron receiving mode and electron repulsion mode (70 eV).

The aforementioned process is attributed to the fact that, in electron repulsion mode, the nonworking filament creates a reverse accelerating electric field for the electrons, which slows them down after they pass through the ionization chamber. Subsequently, the electrons enter the ionization chamber once more, undergoing reverse acceleration and oscillating back and forth between the electron repellers of the two filaments. This phenomenon significantly enhances the probability of collision between the electrons and gas molecules, thereby improving the utilization efficiency of the electrons.

Fig. 5a also illustrates that the signal intensity of the mass spectrum obtained when the electrons oscillate in the electric field is approximately 35% higher than that observed when the electrons do not oscillate, as shown in Fig. 5b. During the actual oscillation process, the

electrons gradually deviate from the central axis, expanding the effective ionization space and allowing for the ionization of more molecules, resulting in a stronger MS peak.

3.2. Experimental comparison of electron oscillation and non oscillation at an electron energy of 35 eV

To investigate the impact of electron oscillation on ionization efficiency in low-energy mode, the electron energy is reduced to 35 eV, and the experiment described in Section 2 is repeated. The experimental findings are presented in Fig. 6a, with electron receiving mode occurring before 40 minutes and electron repulsion mode occurring after 44 minutes.
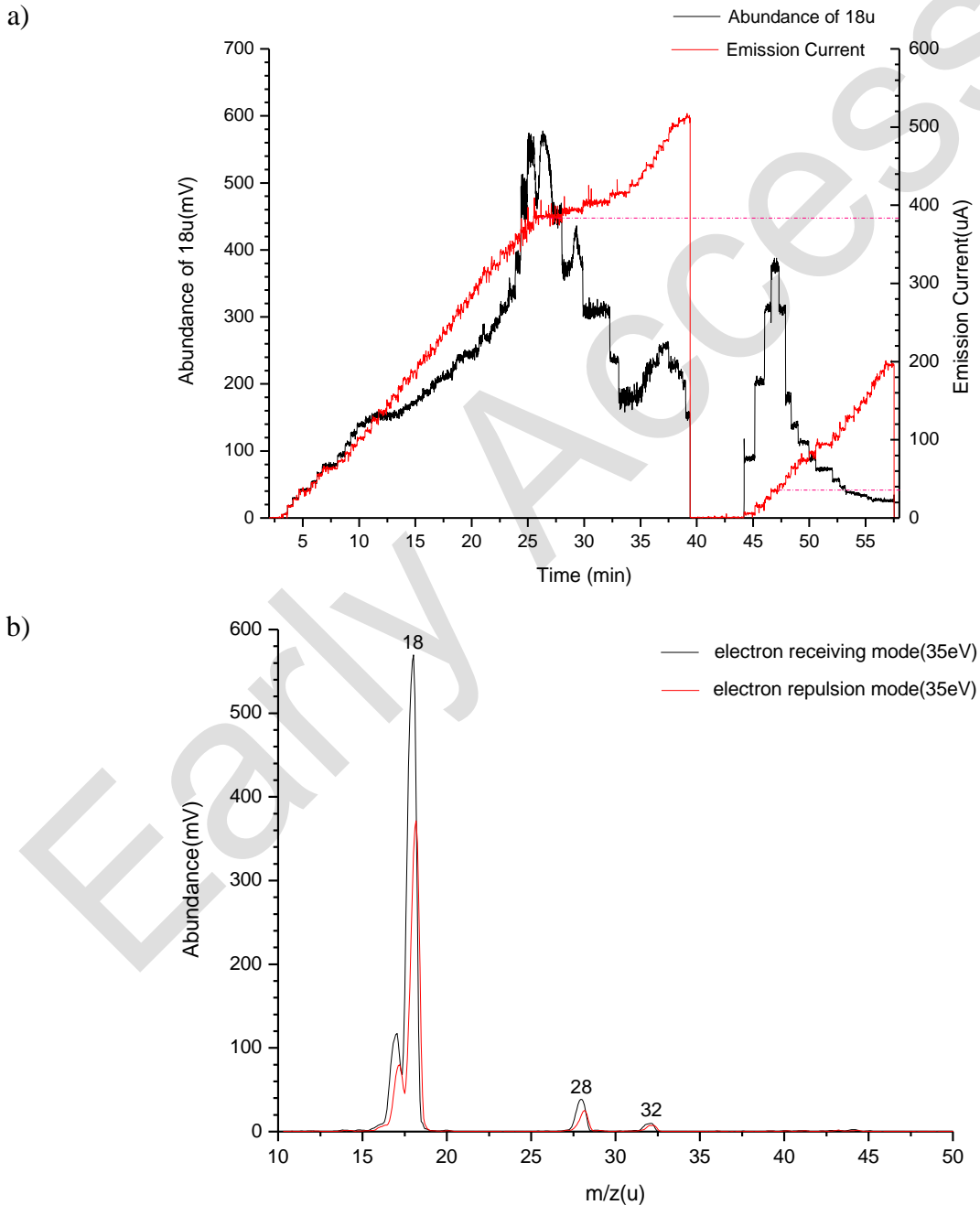

Fig. 6. a) The curve of the filament emission current and m/z 18 intensity at 35 eV (electron receiving mode (< 40 min) and electron repulsion mode (> 44 min). b) Comparison of MS peak intensity in electron receiving mode and electron repulsion mode (35 eV).

When the nonworking filament operates in electron repulsion mode, the emission current required to achieve the strongest MS peak decreases, consistent with the experiment conducted at an electron energy of 70 eV. This result suggests that electron oscillation occurs. However, the emission current needed for maximum MS peak intensity is approximately 380 µA in electron receiving mode and approximately 35 µA in electron repulsion mode. As the electron energy decreases from 70 eV to 35 eV, a higher emission current is required to achieve optimal ionization efficiency due to the weakened electric field force, causing the electrons to diverge more easily. Consequently, the number of oscillating electrons decreases. Additionally, as shown in Fig. 6b, the maximum value of the MS peak obtained during electron oscillation is about 30% lower than that without electron oscillation, which differs from the results observed at 70 eV.

3.3. Experimental comparison of electron oscillation and non oscillation at an electron energy of 15 eV

The electron energy is further decreased to 15 eV, and the experiment is repeated. The findings are presented in Fig. 7, with electron receiving mode occurring before 97 minutes and electron repulsion mode occurring after 98 minutes.

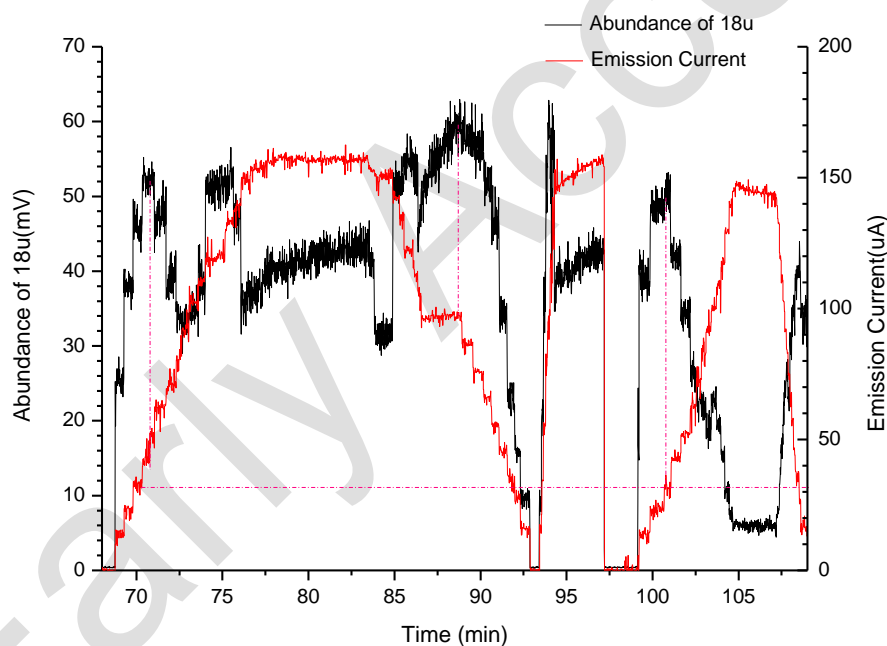Fig. 7. The curve of filament emission current and m/z 18 intensity at 15 eV (electron receiving mode (< 97 min) and electron repulsion mode (> 98 min)).

As the electron energy decreases to 15 eV, the overall abundance of the MS peak further diminishes, and in electron receiving mode, the stability of the MS peak abundance deteriorates. The maximum value of the MS peak fluctuates significantly, particularly when the emission current is relatively high. This phenomenon arises from the fact that lower electron energies result in slower speeds, reducing their ability to pass through the ionization chamber. Additionally, as the electric field weakens, the angle at which electrons deviate from the central axis increases, leading to a more divergent distribution of electron clouds. Consequently, repeatability suffers. In electron repulsion mode, the stability of MS peak abundance is comparatively better, but the difference between repulsion mode and receiving mode regarding the required emission current for maximum MS peak intensity narrows further. This outcome

stems from the decreased number of electrons passing through the ionization chamber. The aforementioned experiments indicate that while electron oscillation can enhance electron utilization, there is an evident downward trend in electron utilization with decreasing electron energy. This reduction is primarily due to the reduced ability of electrons to traverse the ionization chamber as their energy decreases. These findings are also reflected in the experiment presented in Fig. 8. The decrease in electron energy results in a reduced number of electrons that can be received by the receiver. This is likely due to the decreased speed and ability of the electrons to traverse the ionization chamber.
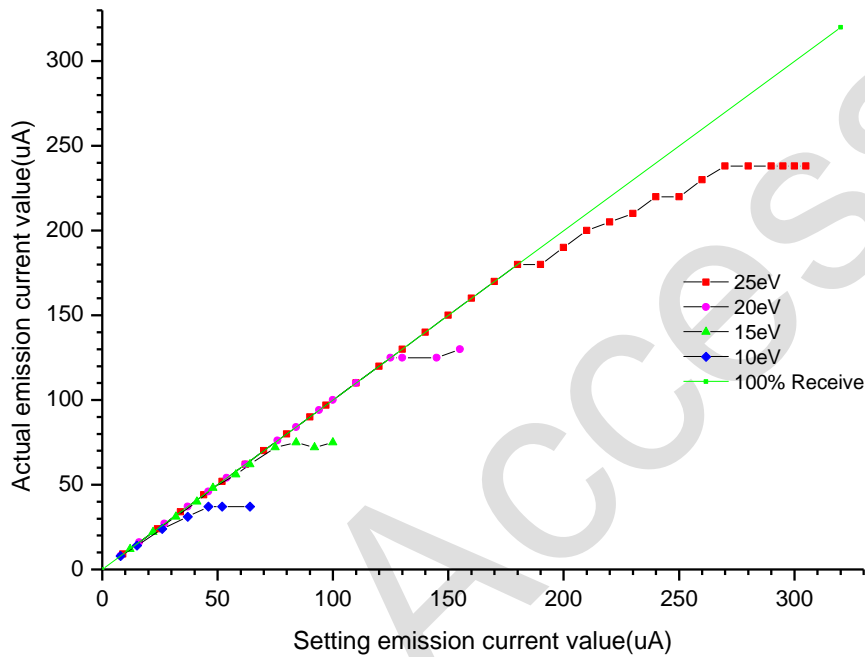

Fig. 8. Curve of the emission current and receiving current at low electron energy.

The primary cause is the reduction in electron energy, which results in a slower speed of electron flight. Consequently, some electrons fail to reach the anode, leading to the accumulation of space charge and the formation of a plane with a natural potential of 0, known as the virtual cathode. To confirm the existence of a virtual cathode, the electron energy was set to 10 eV, and a stable emission current mode was employed. The emission current was set to 64μA, and the actual emission and reception currents were measured, as presented in Table 1. It can be observed that as the voltage of the ion repeller decreases, its impact on the electric field at the filament diminishes. As illustrated in Fig. 9, not all the electrons emitted from the filament are fully received, and some accumulate space charges between the electron repeller and the ionization chamber.
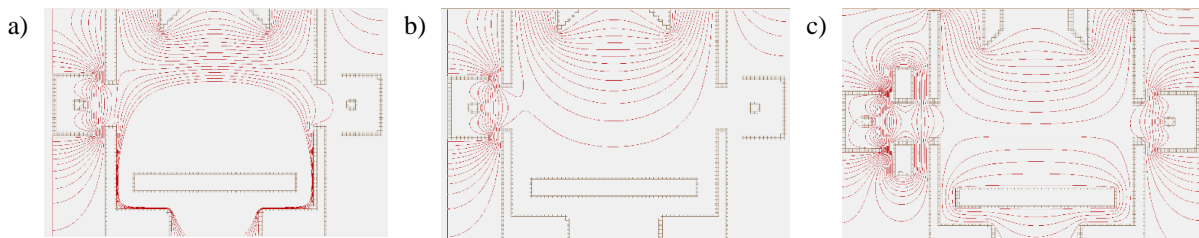

Fig. 9. Distribution of the electric field in the ionization chamber: a) The ion repeller was +50V, while the filament and electron repeller was −10 V, and without electron lens; b) The ion repeller was 0 V, filament and electron repeller was −10 V; c) The ion repeller was +5 V, the filament and electron repeller was −10V, and an electron lens is added.

Table 1 Relationship between the voltage of the electron repeller and the emission and reception currents

Ion repeller voltage (V)	Setting emission current value (μA)	Actual emission current value (μA)	Reception current value (μA)	Electronic reception rate (%)
50	64	64	38	59.38
40	64	64	38	59.38
30	64	64	32	50.00
20	64	52	20	38.46
10	64	38	14	36.84

To eliminate the virtual cathode, an electron lens was incorporated between the filament and the ionization chamber. To assess its impact, the voltage of the electron lens was set to 0V. The resulting electric field distribution is depicted in Fig. 9c. The emission current and reception current were measured again, as presented in Table 2. It can be observed that following the addition of the electron lens, the actual emission current of the filament aligns with the set value, and no space charge is present. The virtual cathode vanishes, significantly enhancing the ability of electrons to traverse the ionization chamber.

Table 2 Relationship between the voltage of the electron repeller and the emission and reception currents

Ion repeller voltage (V)	Setting emission current value (μA)	Actual emission current value (μA)	Reception current value (μA)	Electronic reception rate (%)
50	64	64	40	62.50%
40	64	64	42	65.63%
30	64	64	44	68.75%
20	64	64	46	71.88%
10	64	64	48	75.00%

To further enhance the collisions between electrons and gas molecules, the nonworking filament operates in electron repulsion mode, with the voltage of the electron lens slightly higher than the electron repeller. This allows low-energy electrons to oscillate back and forth within the electric field until they eventually collide with the walls of the ionization chamber and vanish. The integration of electron lenses and electron oscillations significantly improves ionization efficiency at lower electron energies compared to when electron oscillations are absent. As demonstrated in Fig. 10, the MS peak intensity of m/z 18 increased to 4.2 times at 25 eV and to 3.25 times at 20 eV. However, it is also observed that as the electron energy decreases, the attenuation of the MS peak abundance also decreases rapidly. Therefore, in practical applications, a compromise should be made between the ratio of molecular ions to fragments and sensitivity for the selection of electron energy.
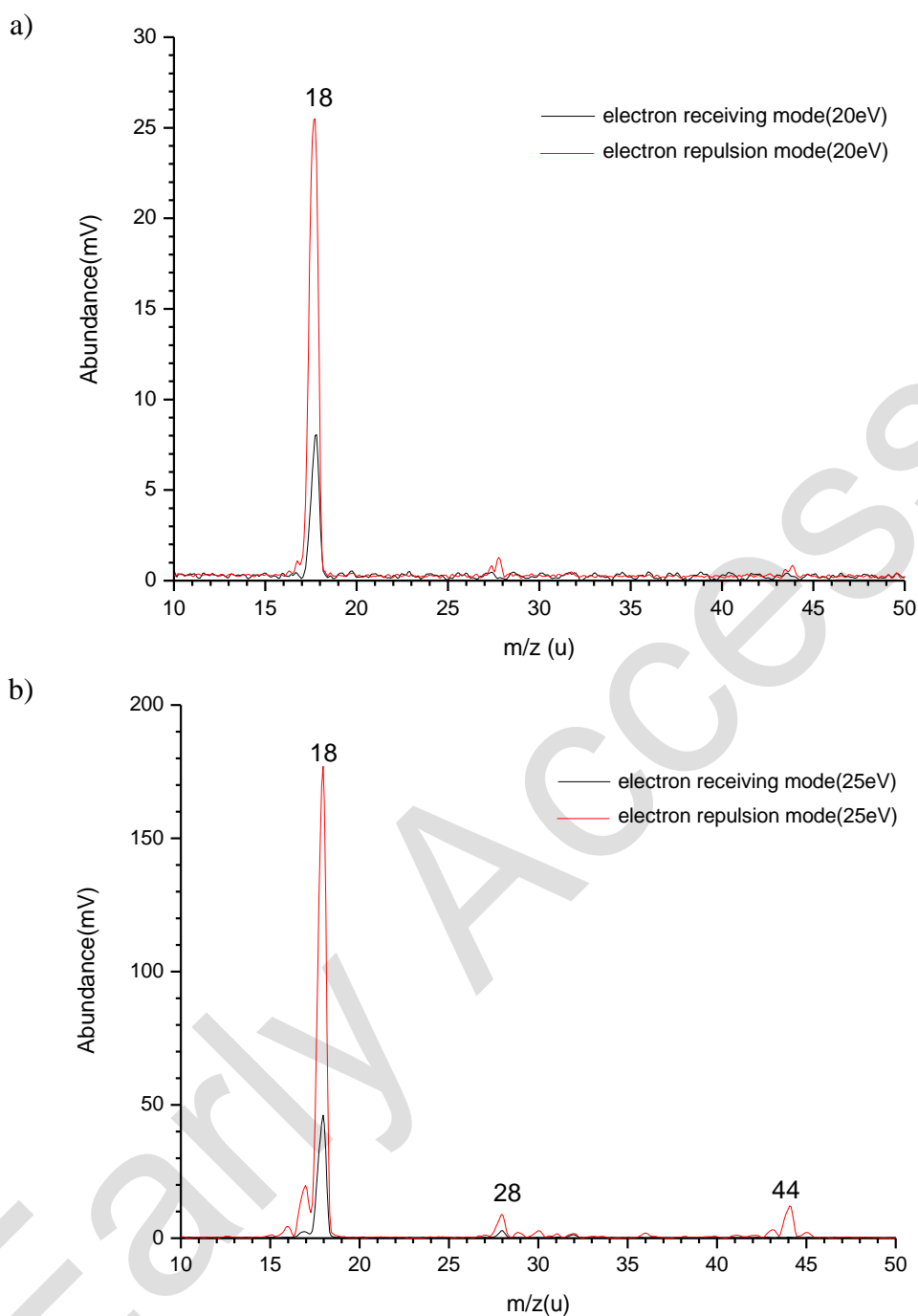
Fig. 10. Enhancement of the MS peak intensity at low electron energy by electron lens and electron oscillation:
a) 20 eV and b) 25 eV.

4. Conclusions

In low electron energy mode, the ionization efficiency of the EI source decreases due to a reduction in collision ionization cross-section. This process significantly impacts the practicality of soft EI. By employing a U-shaped electric field, electrons oscillate back and forth within the ionization chamber, thereby increasing the number of collisions between each electron and gas molecule, effectively enhancing the collision cross-sectional area between them. However, at low electron energies, the emergence of virtual cathode significantly reduces the number of electrons entering the ionization chamber. The introduction of an electron lens greatly improves or even eliminates the virtual cathode effect, resulting in a significant increase

in the number of electrons entering the ionization chamber. When combined with electron oscillation technology, this enhances the ionization efficiency of soft EI, making it more practical and applicable for various purposes, particularly rapid online analysis in process analytical chemistry such as catalyst research and chemical reaction process monitoring. However, the sensitivity at low electron energy in this study still has some gap with that at conventional 70 eV electron energy. Therefore, a lot of theoretical research, experiments and construction work are still needed.

Acknowledgements

References

[1]   Munson, M. S. B., & Field, F. H. (1966). Chemical ionization mass spectrometry. II. Esters. *Journal of the American Society for Mass Spectrometry*, *88*(19), 4337–4345. https://doi.org/10.1021/ja00971a007

[2]   Berresheim, H., Elste, T., Plass-Dülmer, C., Eisele, F. L., & Tanner, D. J. (2000). Chemical ionization mass spectrometer for long-term measurements of atmospheric OH and H2SO4. *International Journal of Mass Spectrometry*, *202*(1-3), 91–109. https://doi.org/10.1016/S1387-3806(00)00233-5

[3]   Hearn, J. D., & Smith, G. D. (2004). A chemical ionization mass spectrometry method for the online analysis of organic aerosols. *Analytical Chemistry*, *76*(10), 2820–2826. https://doi.org/10.1021/ac049948s

[4]   St Clair, J. M., McCabe, D. C., Crounse, J. D., Steiner, U., & Wennberg, P. O. (2010). Chemical ionization tandem mass spectrometer for the in situ measurement of methyl hydrogen peroxide. *Review of Scientific Instruments*, *81*(9). https://doi.org/10.1063/1.3480552

[5]   Fenn, J., Mann, M., Meng, C., Wong, S., & Whitehouse, C. (1989). Electrospray ionization for mass spectrometry of large biomolecules. *Science*, *246*(4926), 64–71. https://doi.org/10.1126/science.2675315

[6]   Fenn, J. B., Mann, M., Meng, C. K., Wong, S. F., & Whitehouse, C. M. (1990). Electrospray ionization – principles and practice. *Mass Spectrometry Reviews*, *9*, 37–70. https://doi.org/10.1002/mas.1280090103

[7]   King, R., Bonfiglio, R., Fernandez-Metzler, C., Miller-Stein, C., & Olah, T. (2000). Mechanistic investigation of ionization suppression in electrospray ionization. *Journal of the American Society for Mass Spectrometry*, *11*(11), 942–950. https://doi.org/10.1016/s1044-0305(00)00163-x

[8]   Smith, R. D., Loo, J. A., Loo, R. R. O., Busman, M., & Udseth, H. R. (1990). Principles and practice of electrospray ionization - mass spectrometry for large polypeptides and proteins. *Mass Spectrometry Reviews*, *10*(5), 359–452. https://doi.org/10.1002/mas.1280100504

[9]   Andrade, F. J., Shelley, J. T., Wetzel, W. C., Webb, M. R., Gamez, G., Ray, S. J., & Hieftje, G. M. (2008). Atmospheric pressure chemical ionization Source. 1. Ionization of compounds in the gas phase. *Analytical Chemistry*, *80*(8), 2646–2653. https://doi.org/10.1021/ac800156y

[10] Andrade, F. J., Shelley, J. T., Wetzel, W. C., Webb, M. R., Gamez, G., Ray, S. J., & Hieftje, G. M. (2008). Atmospheric pressure chemical ionization Source. 2. Desorption−Ionization for the direct analysis of solid compounds. *Analytical Chemistry*, *80*(8), 2654–2663. https://doi.org/10.1021/ac800210s

[11] Cai, S., & Syage, J. A. (2006). Comparison of atmospheric pressure photoionization, atmospheric pressure chemical ionization, and electrospray ionization mass spectrometry for analysis of lipids. *Analytical Chemistry*, *78*(4), 1191–1199. https://doi.org/10.1021/ac0515834

[12] Vogel, A. L., Äijälä, M., Brüggemann, M., Ehn, M., Junninen, H., PetäjÄ, T., Worsnop, D. R., Kulmala, M., Williams, J., & Hoffmann, T. (2013). Online atmospheric pressure chemical ionization ion trap mass spectrometry (APCI-IT-MS<sup>n</sup>) for measuring organic acids in concentrated bulk aerosol – a laboratory and field study. *Atmospheric Measurement Techniques*, *6*(2), 431–443. https://doi.org/10.5194/amt-6-431-2013

[13] Charles, L., Riter, L. S., & Cooks, R. G. (2001). Direct analysis of semivolatile organic compounds in air by atmospheric pressure chemical ionization mass spectrometry. *Analytical Chemistry*, *73*(21), 5061–5065. https://doi.org/10.1021/ac010606l

[14] Chen, H., Lai, J., Zhou, Y., Huan, Y., Li, J., Xie, Z., Wang, Z., & Luo, M. (2007). Instrumentation and characterization of surface desorption atmospheric pressure chemical ionization mass spectrometry. *Chinese Journal of Analytical Chemistry*, *35*(8), 1233–1240. https://doi.org/10.1016/s1872-2040(07)60079-6

[15] Takats, Z., Wiseman, J. M., Gologan, B., & Cooks, R. G. (2004). Mass spectrometry sampling under ambient conditions with desorption electrospray ionization. *Science*, *306*(5695), 471–473. https://doi.org/10.1126/science.1104404

[16] Takáts, Z., Wiseman, J. M., & Cooks, R. G. (2005). Ambient mass spectrometry using desorption electrospray ionization (DESI): instrumentation, mechanisms and applications in forensics, chemistry, and biology. *Journal of Mass Spectrometry*, *40*(10), 1261–1275. https://doi.org/10.1002/jms.922

[17] Cooks, R. G., Ouyang, Z., Takats, Z., & Wiseman, J. M. (2006). Ambient mass spectrometry. Science, *311*(5767), 1566–1570. https://doi.org/10.1126/science.1119426

[18] Zeng, S., Wang, L., Chen, T., Wang, Y., Mo, H., & Qu, H. (2012). Direct analysis in real time mass spectrometry and multivariate data analysis: A novel approach to rapid identification of analytical markers for quality control of traditional Chinese medicine preparation. *Analytica Chimica Acta*, *733*, 38–47. https://doi.org/10.1016/j.aca.2012.04.025

[19] Gross, J. H. (2014). Direct analysis in real time—a critical review on DART-MS. Analytical and Bioanalytical Chemistry, *406*(1), 63–80. https://doi.org/10.1007/s00216-013-7316-0

[20] Petucci, C., Diffendal, J., Kaufman, D., Mekonnen, B., Terefenko, G., & Musselman, B. (2007). Direct analysis in real time for reaction monitoring in drug discovery. *Analytical Chemistry*, *79*(13), 5064–5070. https://doi.org/10.1021/ac070443m

[21] Morlock, G. E., & Chernetsova, E. S. (2012). Coupling of planar chromatography with Direct Analysis in Real Time mass spectrometry. *Central European Journal of Chemistry*, *10*(3), 703–710. https://doi.org/10.2478/s11532-012-0025-2

[22] Wang, Y., Liu, L., Ma, L., & Liu, S. (2014). Identification of saccharides by using direct analysis in real time (DART) mass spectrometry. *International Journal of Mass Spectrometry*, *357*, 51–57. https://doi.org/10.1016/j.ijms.2013.09.008

[23] Nah, T., Chan, M. H., Leone, S. R., & Wilson, K. R. (2013). Real time in situ chemical characterization of submicrometer organic particles using direct analysis in Real Time-Mass spectrometry. *Analytical Chemistry*, *85*(4), 2087–2095. https://doi.org/10.1021/ac302560c

[24] Na, N., Zhao, M., Zhang, S., Yang, C., & Zhang, X. (2007). Development of a Dielectric Barrier Discharge Ion Source for Ambient Mass Spectrometry. *Journal of the American Society for Mass Spectrometry*, *18*(10), 1859–1862. https://doi.org/10.1016/j.jasms.2007.07.027

[25] Hiraoka, K., Ninomiya, S., Chen, L. C., Iwama, T., Mandal, M. K., Suzuki, H., Ariyada, O., Furuya, H., & Takekawa, K. (2011). Development of double cylindrical dielectric barrier discharge ion source. *Analyst*, *136*(6), 1210. https://doi.org/10.1039/c0an00621a

[26] Hiraoka, K., Chen, L. C., Iwama, T., Mandal, M. K., Ninomiya, S., Suzuki, H., Ariyada, O., Furuya, H., & Takekawa, K. (2010). Development of a Remote-from-Plasma dielectric barrier discharge ion source and its application to explosives. *Journal of the Mass Spectrometry Society of Japan*, *58*(6), 215–220. https://doi.org/10.5702/massspec.58.215

[27] Butcher, D. J. (1999). Vacuum Ultraviolet Radiation for Single-Photoionization Mass Spectrometry: A Review. *Microchemical Journal*, *62*(3), 354–362. https://doi.org/10.1006/MCHJ.1999.1745

[28] Kang, W. J., Teepe, M., Neyer, A., Baumbach, J. I., Schmidt, H., & Sielemann, S. (2001, January). In Miniaturized Ion Mobility Spectrometer (µIMS) with UV-Lamp as a Photoionization Source, *ISIMS 200110th Int. Conf. on Ion Mobility Spectrometry*.

[29] Syage, J. A., & Evans, M. D. (2001). Photoionization mass spectrometry - A powerful new tool for drug discovery. *Spectroscopy Springfield Then Eugene Then Duluth*, *16*(11), 14–18.

[30] Luosujärvi, L. (2010). *Miniaturized mass spectrometric ionization techniques for environmental analysis and bioanalysis* [Academic Dissertation, University of Helsinki]

[31] Eschner, M., Gröger, T., Horvath, T. D., Gonin, M., & Zimmermann, R. (2011). Quasi-Simultaneous Acquisition of Hard Electron Ionization and Soft Single-Photon Ionization Mass Spectra during GC/MS Analysis by Rapid Switching between Both Ionization Methods: Analytical Concept, Setup, and Application on Diesel Fuel. *Analytical Chemistry*, *83*(10), 3865–3872. https://doi.org/10.1021/ac200356t

[32] Capozza, G., Segoloni, E., Leonori, F., Volpi, G. G., & Casavecchia, P. (2004). Soft electron impact ionization in crossed molecular beam reactive scattering: The dynamics of the O(3P)+C2H2 reaction. *The Journal of Chemical Physics*, *120*(10), 4557–4560. https://doi.org/10.1063/1.1652013

[33] Yang, S., Brereton, S. M., Wheeler, M. D., & Ellis, A. M. (2006). Soft or hard ionization of molecules in helium nanodroplets? An electron impact investigation of alcohols and ethers. *Physical Chemistry Chemical Physics*, *7*(24), 4082–4088. https://doi.org/10.1039/b511628g

[34] Amirav, A., Keshet, U., & Danon, A. (2015). Soft Cold EI – approaching molecular ion only with electron ionization. *Rapid Communications in Mass Spectrometry*, *29*(21), 1954–1960. https://doi.org/10.1002/rcm.7305

[35] Gordin, A., Fialkov, A. B., & Amirav, A. (2008). Classical electron ionization mass spectra in gas chromatography/mass spectrometry with supersonic molecular beams. *Rapid Communications in Mass Spectrometry*, *22*(17), 2660-2666. https://doi.org/10.1002/rcm.3654

[36] Alon, T., & Amirav, A. (2015). How enhanced molecular ions in Cold EI improve compound identification by the NIST library. *Rapid Communications in Mass Spectrometry*, *29*(23), 2287-2292. https://doi.org/10.1002/rcm.7392

[37] Khare, P., Marcotte, A., Sheu, R., Ditto, J., & Gentner, D. R. (2017, December). Next generation offline approaches to trace organic compound speciation: Approaching comprehensive speciation with soft ionization and very high resolution tandem mass spectrometry. American Geophysical Union.

[38] Ehrhardt, H., Jung, K., Knoth, G., & Schlemmer, P. (1986). Differential cross sections of direct single electron impact ionization. *Zeitschrift Für Physik*, *1*(1), 3–32. https://doi.org/10.1007/bf01384654

[39] Straub, H. C., Renault, P., Lindsay, B. G., Smith, K. A., & Stebbings, R. F. (1996). Absolute partial cross sections for electron-impact ionization of H_2, N_2, and O_2 from threshold to 1000 eV. *Physical Review A*, *54*(3), 2146-2153. https://doi.org/10.1103/PhysRevA.54.2146

[40] Straub, H. C., Renault, P., Lindsay, B. G., Smith, K. A., & Stebbings, R. F. (1995). Absolute partial and total cross sections for electron-impact ionization of argon from threshold to 1000 eV. *Physical Review A*, *52*, 1115-1124. https://doi.org/10.1103/PhysRevA.52.1115

[41] Lindsay, B. G., Merrill, R. L., Straub, H. C., Smith, K. A., & Stebbings, R. F. (1998). Absolute differential and integral cross sections for charge transfer of keV O+ with N2. *Physical Review A*, *57*, 331. https://doi.org/10.1103/PhysRevA.57.331

[42] Deutsch, H., Becker, K., Matt, S., & Märk, T. D. (2000). Theoretical determination of absolute electron-impact ionization cross sections of molecules. *International Journal of Mass Spectrometry*, *197*(1), 37-69. https://doi.org/10.1016/S1387-3806(99)00257-2

[43] Ye, M. Y., & Takamura, S. (2000). Effect of space-charge limited emission on measurements of plasma potential using emissive probes. *Physics of Plasmas*, *7*, 3457–3463. https://doi.org/10.1063/1.874210

[44] Tierno, S. P., Donoso, J. M., Domenech-Garret, J. L., & Conde, L. (2016). Existence of a virtual cathode close to a strongly electron emissive wall in low density plasmas. *Physics of Plasmas*, *23*, 013503. https://doi.org/10.1063/1.4939042

[45] Takamura, S., Ohno, N., Ye, M. Y., & Kuwabara, T. (2004). Space-charge limited current from plasma-facing material surface. *Contributions to Plasma Physics*, *44*, 126–137. https://doi.org/10.1002/ctpp.200410017

[46] Marek, A., Jílek, M., Picková, I., Kudrna, P., Tichý, M., Schrittwieser, R., & Ionita, C. (2008). Emissive probe diagnostics in low-temperature plasma - effect of space charge and variations of electron saturation current. *Contributions to Plasma Physics*, 48, 491–496. https://doi.org/10.1002/ctpp.200810079

[47] Intrator, T., Cho, M. H., Wang, E. Y., Hershkowitz, N., Diebold, D., & Dekock, J. (1988). The virtual cathode as a transient double sheath. *Journal of Applied Physics*, 64, 2927–2933. https://doi.org/10.1063/1.341552

[48] Li, S.-h., & Li, J.-q. (2021). Studies of virtual cathode characteristics near thermionic emission cathodes in a vacuum. *Vacuum*, 192, 110496. https://doi.org/10.1016/j.vacuum.2021.110496

[49] Huang, Z. J., Jiang, Y., Yue, J. R., Gong X.-Yun, Liu M. Y., Fang X. (2018). Design and Test for On-Line Rapid Process Mass Spectrometer. *Journal of Chinese Mass Spectrometry Society*, *39*(4), 399-406. https://doi.org/10.7538/zpxb.2017.0149

Zejian Huang holds a PhD in Physical Chemistry from Fudan University and currently serves as a senior researcher at the National Institute of Metrology in China. His research primarily revolves around the miniaturization of mass spectrometers and the development of online mass spectrometry technology. Dr. Huang has been granted 24 Chinese invention patents and 3 US patents, and has received numerous accolades for his work, including a second prize from the National Science and Technology Progress Award, a first prize from the Science and Technology Revitalization Award of the General Administration of Quality Supervision, Inspection, and Quarantine of the People's Republic of China, and two first prizes from the Science and Technology Award of the China Instrument and Meter Association.

You Jiang earned his Ph.D. from Jilin University in 2008 and is currently a research professor at the National Institute of Metrology in China, where he also serves as the director of the Laboratory of Mass Spectrometry. Dr. Jiang has published more than 30 journal articles and holds 20 issued patents. He has been honored with the second prize of the National Science and Technology Progress Award twice. His current research focuses on chemical and biometrical measurements, mass spectrometry principles, instrumental engineering, and control technologies.

XinHua Dai earned her Ph.D. from the Institute of Chemistry of the Chinese Academy of Sciences in 2004 and is currently a senior researcher, vice president of the National Institute of Metrology in China, chairman of the National Biometrology Technology Committee, and vice chairman of the National New Materials and Nanometrology Technology Committee. Dr. Dai has authored or co-authored over 100 journal articles and has been awarded the second prize of the National Science and Technology Progress Award three times. Her current research focuses on life science metrology, mass spectrometry technology, and metrology technology management.

Mingfei Zhou obtained the Ph.D. degree from Fudan University in 1995 and stayed on as a teacher after graduation. Currently, he is a professor and head of the Department of Chemistry at Fudan University. From 1997 to 1999, he engaged in postdoctoral research in the Department of Chemistry at the University of Virginia in the United States. He was promoted to professor in 2000 and was supported by the National Science Foundation for Distinguished Young Scholars in 2001. In 2002, he was appointed as a Changjiang Distinguished Professor. Mainly engaged in molecular spectroscopy and chemical bond research. In Science, Nature, Angelw Chem Int. Ed. and J. Am. Chem More than 320 papers have been published in academic journals such as Soc. As the first adult, he won the first prize of Shanghai Natural Science Award (2007) and the second prize of National Natural Science Award (2018). He was selected as a member of the American Physical Society in 2019 and the Chinese Chemical Society in 2020.

Xiang Fang is currently a senior researcher, serving as the president of the National Institute of Metrology in P.R. China and as a member of the executive committee of the Asia Pacific Metrology Programme (APMP). He has authored or coauthored over 50 journal articles and holds 32 issued patents. In recognition of his contributions to science and technology, he has been awarded the second prize of the National Science and Technology Progress Award twice. Xiang Fang's current research interests include chemistry, biometric measurement, theoretical study of mass spectrometry, and instrument engineering technology. His expertise and dedication to these fields have made him a respected figure in the scientific community.